Journal of Remanufacturing (2024) 14:293–314
https://doi.org/10.1007/s13243-024-00146-3

RESEARCH

Flattening of bent metal sheets as a remanufacturing operation

Daniele Farioli[1] · Ertugrul Kaya[1] · Matteo Strano[1]

Received: 6 May 2024 / Accepted: 20 November 2024 / Published online: 4 December 2024

Abstract
The reshaping of end-of-life or scrap sheet metal panels is a potential remanufacturing process, which enables significant environmental benefits over the traditional metal recycling routes. This paper experimentally investigates cold and warm press flattening of waste sheet metal for enabling remanufacturing. Samples of stainless steel, aluminium alloy, and low carbon steel were bent to various internal angles using v-die air bending operations. Then, flattening tests were conducted with a hydraulic press, with tools capable of heating up to 300 °C. The process parameters included dwell force, dwell time, and tool temperature. The target final angle after load release is set at 180°, but the flattening process typically induces springforward, and the final angle is generally larger than 180°. Springforward can be mitigated by using warm flattening conditions with all the tested materials. It can also be reduced if superposing a steel mesh between the top flattening die and the sheet. The paper demonstrates and explains the mechanical effects of the flattening process.

Keywords Remanufacturing · Warm forming · Sheet metals · Springforward

Introduction

Traditional business models typically adhere to a linear "make-use-dispose" approach. However, there is a growing shift towards embracing circularity, which entails the continuous circulation of materials and products, offering environmental and economic benefits. This transition is facilitated through either open-loop or closed-loop supply chains, where materials or products undergo processes like recycling, repurposing, or remanufacturing

✉ Matteo Strano
matteo.strano@polimi.it

Daniele Farioli
daniele.farioli@polimi.it

Ertugrul Kaya
ertugrul.kaya@polimi.it

[1] Dipartimento di Meccanica, Politecnico di Milano, via La Masa 1, 20156 Milan, Italy

[1]. The effectiveness of these approaches varies, and depending on the specific case, they may yield greater advantages in terms of economics, environmental sustainability, or social impact. The remanufacturing of used products is conventionally defined as the restoration of a product to the same specifications as the corresponding new product [2]. Repurposing refers to finding new uses for end-of-life (EoL) products [3]. Sheet metal recycling is traditionally conducted through remelting of collected, shredded and sorted waste. A more environmentally sustainable route for recycling metals is by doing it at the solid state [4], e.g. by consolidation of shredded metal chips (mostly made of aluminium) [5]. The consolidation can be obtained by several methods such as hot extrusion [6], friction stir processing [7] or compaction assisted by spark plasma sintering [8]. Reference [9] provides a concise overview and categorization of the previously mentioned strategies. It explores advancements in sustainable metal production, shifting from raw material efficiency to a more holistic approach that prioritizes materials for reuse, remanufacturing, and recycling. The work identifies four key strategies for enhancing sustainability: reusing metal without melting, reducing material use while maintaining performance, extending product lifespan, and optimizing heat management and supply chains to lower CO2 emissions. Additionally, it outlines several "R-strategies" aimed at improving material lifecycle management:

1. **Reusing**: Utilizing metal products without melting them down.
2. **Reducing**: Using less metal while maintaining functionality.
3. **Repairing**: Extending product lifespans through repairs.
4. **Remanufacturing**: Restoring used products to like-new condition.
5. **Recycling**: Processing end-of-life materials to reclaim value while minimizing losses.

The reProd® approach provides a sustainable alternative to linear economic models by shortening the cycle from used products to new semi-finished ones, reducing waste and energy use. It promotes a circular economy, extending material use and lowering environmental impact.

Reshaping can be viewed as a form of remanufacturing, as it allows for the restoration and optimization of a product's original characteristics, thereby extending its useful life. Recently, the reshaping of relatively large EoL sheet metal panels has been proposed by a few authors as an innovative way which can be considered halfway between solid state recycling and remanufacturing. In fact, the EoL part is not shredded and transformed into a new secondary raw material, but it is directly transformed into a new sheet metal part. The reshaping of end-of-life or scrap sheet metal panels enables significant environmental benefits over the traditional metal recycling routes [10]. Single point incremental forming can be used as a flexible technology, to this purpose [11], exploiting the large formability yielded by this technique. Other authors proposed the use of nearly flat sheet metal scraps to produce facade components by cutting, punching and bending operations [12]. Facade elements made of sheet metals can be implemented with innovative concepts offering multifunctional advantages [13], and are particularly suited for remanufacturing applications because they do not require strict surface aesthetical or mechanical properties. Conventional deep drawing can be used as a method for producing a new sheet metal part, starting from an EoL blank which is already nearly flat, such as the roof of a car [14]. Also sheet hydroforming has been proposed as a remanufacturing technique, starting from an EoL car hood [15]. Another possibility is to transform stretched and flattened sheet metal fragments

into mesh sheet for various potential applications [16]. While reshaping operations can be performed directly onto waste sheets with a generic shape, doing it on a nearly flattened shape obviously facilitates any subsequent remanufacturing operation. A waste sheet metal fragment can be considered a good candidate for remanufacturing if it has enough residual formability [17, 18], if it is large enough for the remanufactured part, if its thickness distribution is within a prescribed tolerance. Flattening is therefore a useful, environmentally inexpensive, preliminary operation before the new shape is given to the remanufactured part. It could be performed thermally, i.e. by laser flattening [19], if a localized irregularity must be removed. More effectively, it can be performed by applying mechanical pressure, e.g. by roll levelling [20], when the scrap sheet is not previously severely deformed. Finally, sheet metal scraps can be flattened at a press equipped with flat upper and lower tools [21]. The outcome of a press flattening operation primarily depends of the initial shape and size of the sheet metal scrap and the main problems that prevent a successful flattening operations are elastic springback [22] and springforward [23]. While springforward is very rare in direct forming processes and first-step forming operations, as it will be shown later, it is very frequent in flattening and unbending steps.

The reduction or suppression of springback phenomena, in sheet metal forming, can be obtained by means of local or global stress superposition, in a direction different to the stress direction that generates the springback. This approach has been used and demonstrated in air bending [24], but also in deep drawing [25], in tube bending [26] and in other forming processes [27]. Local stresses can be superposed in different ways, including by a macro-structuring of the tools surfaces, i.e. by using tool with dented or grooved surfaces. Springback suppression by macro-structuring the tools has mostly been applied, in the scientific literature, to the surface of the blankholder [28], which does not influence the surface quality of the formed part. However, it has been demonstrated that a so-called anticlastic curvature of the sheet metals (i.e. a curvature in a direction different to the bending direction) significantly reduces springback [29]. The presence of grooves or dents on a forming tool (a punch or a die) generates anticlastic curved feature, that dramatically reduces springback. This concept has been tested, in the scientific literature, only by two papers presented at the IDDRG Conference in year 2016 [30] and year 2022 [31], where deep drawing punch/die sets were modified by adding stiffening beads. It has never been tested, to the authors' knowledge, in bending nor in press flattening operations.

Among the different geometrical features that can be found in EoL parts, particularly difficult to be flattened are what the auto body makers call the "design lines" or "feature lines", i.e. narrow and long curved features on a smooth panel, bent to a relatively sharp bending radius [32]. A preliminary study has been conducted on EoL aluminium sheets, showing that warm flattening can be effective to flatten out the design lines of real auto body aluminium panels [33]. The purpose of the present paper is to demonstrate the role of the main press flattening parameters (contact pressure and tool temperature) when trying to unbend v-shaped sheet metal rectangular specimens, representative of design lines. The results of an extensive plan of experiments, conducted on different bend geometries, materials and thicknesses will be described. Besides, the superposition of a metal grid between the tools and the sheet metal parts will be shown to be able of nearly suppressing springback and springforward phenomena also for the most challenging conditions.

Table 1 Characteristics of the samples used in bending and flattening tests

		Stainless steel		Low carbon steel	Aluminium alloy	
Initial geometry	thickness t_0 (mm)	0.8	1.2	0.8	0.8	1.2
	length L (mm)	200	200	265	200	200
	width w (mm)	50	50	103	50	50
Material properties	Yield stress s_0 (MPa)	333	264	246	110	136
	Tensile strength s_f (MPa)	1049	1010	394	260	274
	K (MPa)	1478	1434	502	354	368
	e_0	0.0020	0.0015	0.0015	0.0015	0.0020
	n	0.24	0.26	0.11	0.18	0.16

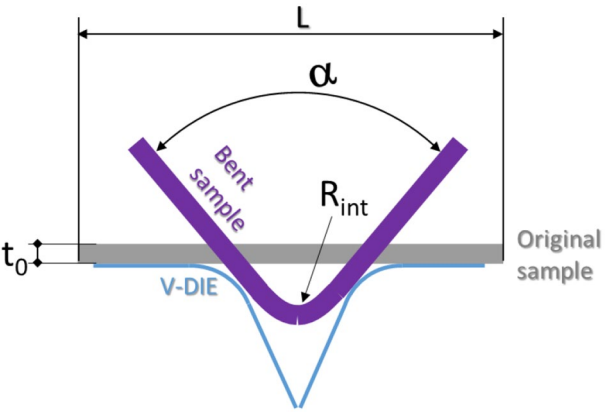

Fig. 1 Dimensions of original and bent samples, initial length L, internal bend angle α, internal radius R_{int}, initial thickness t_0

Materials and methods

Specimen materials and bent geometries

Several samples of rectangular size (length L, width w, initial thickness t_0 and planar surface S=L*w), from three different incoming cold rolled sheet metals have been preliminary bent to various target internal bend angles a, through v-die air bending [34] operations. The materials are: stainless steel AISI 304, aluminium alloy Al 5754, low carbon steel DC04. The material properties have been determined through tensile tests and the hardening parameters (K, e_0 and n) of the Krupkosky's law [35]:

$$\bar{\sigma} = K\left(\varepsilon_0 + \bar{\varepsilon}\right)^n \tag{1}$$

have been determined. The properties and thickness values of all sample types are listed in Table 1, the dimensions are defined in Fig. 1. The punch is made of tool steel with a tip radius of 0,8 mm and the die has an opening width of 10 mm. Other dimensions of the tools are given in Table 2. One can expect that stronger and thicker sheets should be more difficult to be flattened, and this is the reason why different materials and thicknesses have been tested.

Table 2 Mean bent internal radii R_{int} and bent angles α

Material		Stainless steel			Low carbon steel	Aluminium alloy		
Bending tooling	Punch and die tip angle (°)	60	88	88	88	60	88	88
	Die corner radius (mm)	1	2	2	2	1	2	2
Bent angle	Mean bent angle α (°)	75	120	165	103	75	120	165
	Coefficient of variation cov	0.37%	1.13%	0.37%	2.6%	0.30%	0.73%	0.3%
Bent radius	Mean internal radius R_{int} (mm)	1.74	2.57	9.85	5.05	1.16	2.07	10.58
	Coefficient of variation cov	4%	6%	12%	3%	17%	10%	9%

The specimens have been bent to the mean angles a, listed in Table 2, ranging from 75° to 165°. It is predictable that samples bent to smaller angles should be more difficult to be flattened. The actual values of α have been obtained with a coefficient of variation cov (which is the ratio between the standard deviation and the mean) which is also reported Table 2, ranging from 0,3% to 2,6%. The resulting internal radius R_{int} of the bent sheets is reported too, ranging from 1.2 to 10.6 mm. Experimentally, the internal radius has been computed by first measuring the external radius R_{ext}, on the extrados of the bend (which is easier to be measured), and then subtracting the actual thickness of the specimen: $R_{int}= R_{ext} - t_0$.

The surface extension S_b of the bent region of each sample has been estimated with the simple equation:

$$S_b = w \cdot \alpha \cdot R_{ext} \tag{2}$$

where α is given in radians and w is the sample width.

Considering that each experimental condition has been replicated multiple times, a total of 82 samples has been bent, measured and then subsequently flattened, as described in sect. "Press flattening tests".

Press flattening tests

Flattening can be considered as a remanufacturing process, by reshaping pre-formed parts for potential reuse. Flattening tests have been conducted with a single effect hydraulic press, with a maximum tonnage of 400 tons. The upper and lower tools can be heated up to 300 °C by means of electric resistance cartridges embedded in heated plates. The upper and lower tools are simply flat tool steel dies (Fig. 2a). The flattening process is characterized by three main parameters: the dwell force F (tons), the dwell time τ (s), the tool temperature T (°C).

The dwell force F is the maximum flattening force applied during each process. Figure 2b well explains the press flattening cycle. The first phase is where most of the flattening occurs, the sheet is unbent with only three points of contact and the pressing force is very limited (around 20 tons, which is the minimum load that the press can provide). While flattening, the upper die moves down at a constant and controlled slow rate (120 mm/min). When the upper tool approaches the sheet thickness, i.e. when the sheet is nearly flat, the contact surface becomes large, a compression phase starts with the load rapidly increasing and the tool decelerating. When the predetermined dwell force value F is reached (close to 250 tons in the example given in the figure), the tool stops its movement and the load is kept

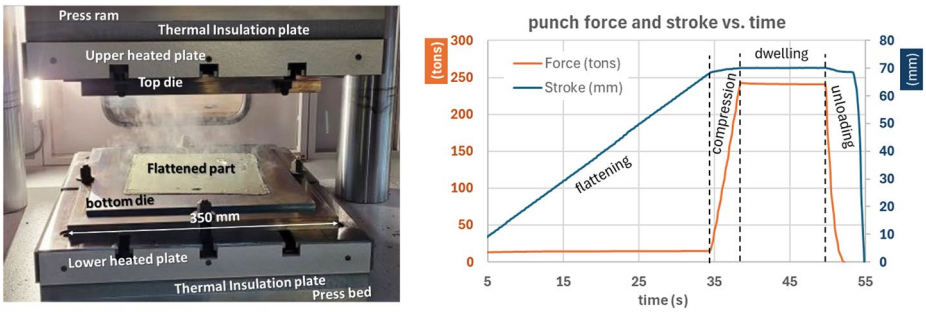

Fig. 2 (**a**) the tooling setup shown at the end of a hot flattening operation of an aluminium panel taken from an EoL car body part; (**b**) typical force and displacement vs. time plot of a flattening test of a v-die bent sample

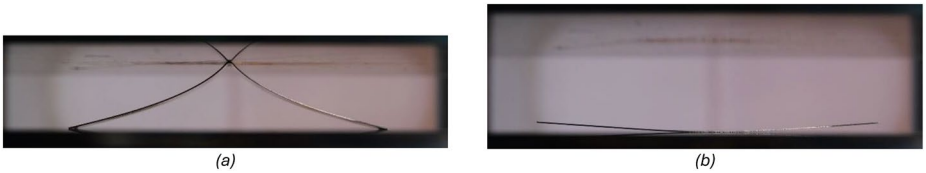

Fig. 3 Sequence of deformation during a flattening test; (**a**) while flattening the flanges mildy bend upward, (**b**) after unloading unloading the flanges lift upward, with a sprignfarward phenomenon

constant for a set time, called dwell time τ (t is equal to 10 s in the given example and also in all tests described in the present study). Finally, the ram moves upwards to return at the original position, causing the load to decrease and becoming null, thus allowing the sheet to either springback or springforward.

In Fig. 3 the shape of a bent specimen under flattening is shown, at different pressing phases shown in Fig. 2b. During the test the two flanges of the sample, which are initially flat, become mildly bent with an upward curvature (Fig. 3a). As a consequence, the ends of the specimen lift upward as the upper tool continues its movement and this is the cause of a springforward phenomenon (Fig. 3b).

The final shape of the sample, after the load has been released, is not perfectly flat, since both springback and springforward phenomena take place. Springback obviously occurs at the initially bent region, i.e. at the centre of the sample. That region is unbent during dwelling, i.e. the angle a is brought to nearly 180°, and when the load is released a partly returns to its original value. Immediately to the left and to the right of the central bending region, the flanges are curved in an opposite direction, as shown in Fig. 3c. As a result, the central part of the specimen, after unloading, is left with a typical m-shaped profile (Fig. 4a) and the flanges may remain lifted upward, thus generating a final springforward shape.

To reduce or even suppress the occurrence of springback and springforward, a possible remedy is to apply, during dwelling, a superposition of local stresses trough stiffening beads. For this reason, during some of the flattening tests, a steel mesh has been placed between the top flat tool and the v-bent sample before pressing. The steel mesh is made of round wires with a diameter of 1.5 mm, sized to form square elements of 13 mm side length (Fig. 4b).

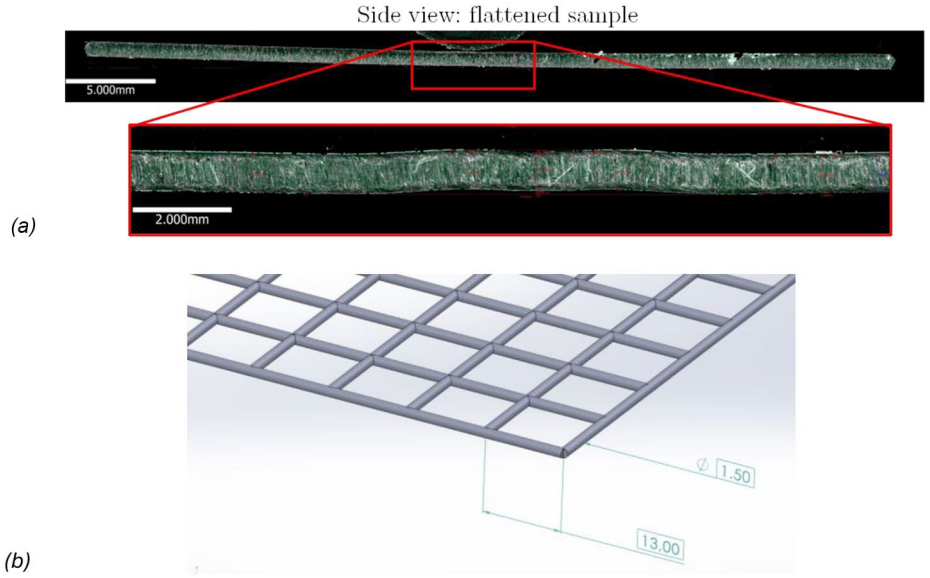

Fig. 4 (**a**) residual m-shaped profile of a specimen after bending and flattening. The sample is observed transversally with an otpical microscope; (**b**) dimension of the steel mesh used in flattening tests with stress superposition

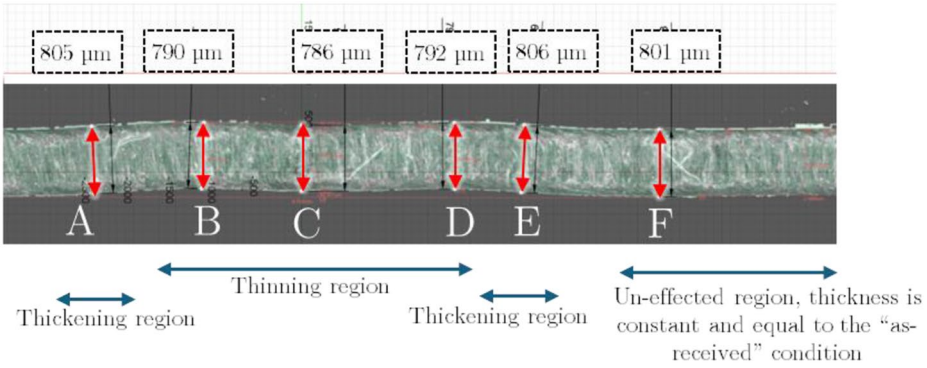

Fig. 5 Measurement of the thickness distribution of the sample bent and flattened

Analysing more in details Fig. 4a through the embedded software of Alicona Infinite Focus, it is possible to determine the thickness in different points of the specimen as represented in Fig. 5. More precisely it is possible to highlight three regions:

– Unaffected regions "far" from the bent line, which maintains the original thickness (point F).
– A thinning region, exactly in the middle of the sample (points B, C and D). Thinning occurs because of the first bending stage, where the material is stretched.

– A small thickening region, located between the thinning and unaffected areas (points A and E), arises from the flattening process. This transition zone results from an unbending phenomenon that creates an "M" shape profile, while the localized pressure from the dies near points B and D causes slight material spreading at points A and E, where thickening occurs. This effect manifests during the final stages of flattening, where friction limits the lateral spreading and deformation of the central portion of the sample.

The concept of real contact surface Sc

In the context of a flattening process, such as when a V-bent metal part undergoes flattening with a flat hard tool, the real contact surface refers to the actual area of contact between the flattened surface of the workpiece and the tool. It is well known that in flattening operations the contact pressure is not uniform, and that there are regions of the specimen which are not in real full contact with both tools [36]. The real contact area S_c is often smaller than the apparent contact area S, because of a non-perfect planarity of the sheet during dwelling. For instance, in parts with a larger initial curvature radius (and larger bending angles) the contact surface between the outer skin of the metal sheets and the flattening die is larger than if flattening a sharp bent, where the pressure will be localized in a small location.

The real contact surface is critical for several reasons. It impacts the **pressure distribution** and the **quality of the finished part** after flattening; a larger contact area can lead to better distribution of forces, reducing localized stresses and lead to fewer aesthetical defects. On the other hand, a smaller contact surface induces a larger real contact pressure and therefore it can have a more effective flattening effect.

During dwelling with flat dies, the mean nominal pressure P applied to the specimen is simply equal to P=F/S, where S is the specimen surface. However, S is only an apparent contact surface, while the real contact surface S_c can only be estimated by means of an analytical or numerical or empirical model. In a v-bent specimen, the regions of the specimen which will be more likely under pressure are the bent region (surface S_b) and the right and left ends of the rectangular sample. An empirical rule of thumb for estimating the real contact surface has been developed by analysing the results of FEM simulations of the process (which will be presented in sect. "Discussion of the effects of using a steel mesh through numerical simulations"). The FEM have shown that the right and left sheet flat ends which are under high contact pressure during dwelling represent about 25% of the total sheet surface S. The FEM results have also shown that at the centre of the sample, because of the M-shape which is taken (as discussed above), the actual contact area is smaller than the bent surface S_b, approximately 82,5% of it. Therefore, the real contact surface S_c has been roughly estimated with the following empirical equation:

$$S_c = 0.825S_b + 0.25S \tag{3}$$

As a consequence the actual mean contact pressure P is estimated as:

$$P = {}^{F}\Big/_{S_c} \tag{4}$$

The flattening tests have been planned with different levels of dwelling pressure P. The actual pressure ranges tested for each material and thickness are summarised in Table 3.

The tests have also been planned with different levels of tool temperature T. A hot level has been set as 50% of the materials melting point: T_{hot}=0,5*T_m; a warm intermediate level has been set as 19% of the melting point: T_{warm}=0,19*T_m; a cold level T_{room} has been set with the tool at the room temperature. Since the maximum available temperature at the tools is 300 °C, the hot level has only been tested for the aluminium alloy, because T_{hot} for the steels would exceed 300 °C. The resulting values are summarised in Table 3.

Measurement of results

The main response of each flattening test has been assessed by measuring the final angle α_f (°) of the sheet, after unloading. The target α_f value is obviously 180 °, with a perfectly planar surface. While the initial angle of the bent sheet is relatively easy to measure, even with a manual goniometer, the final angle is not, because the flattened top surface of the sheet may present large and uneven curvature radii. For this reason, an automatic measurement device has been used. It is a blue laser profilometer (by Wenglor), mounted onto a linear slider; it scans a line in the X direction and it travels at constant speed in the Y direction. The scanner can measure the position of the top sheet surface, with a scanning area (50×250 mm) that completely includes the width w of the specimens used in this study. It has a resolution of 0,5 mm both in the X and Y horizontal directions, but it has a very fine vertical resolution of 0.002 mm.

A colormap of a scanned sample, flattened with flat tools, is shown in Fig. 6a; A longitudinal cross-section of the scanned sample is also shown in the figure. The specimen is bent in the opposite direction of the initial v-die bent sample, i.e. it underwent springforward. At the bottom of the flattened sample, where the original bend line was, an m-shaped profile is evident, with 2 curvature changes. The plot in Fig. 6b can be used to compute the final angle α_f, through a matlab script. The final angle angle α_f for this specimen is 187.9°, with a springforward of nearly 8° from the flat angle of 180°.

A colormap is shown in Fig. 7a, representing the position of the top surface in a sample flattened with the top tools equipped with the stiffening steel mesh pictured in Fig. 4; the colormap highlights very well the suppression of springback and springforward allowed by the grid, while obviously producing a sample with a regularly indented thickness profile. The final angle angle α_f for this specimen is nearly 179,7° (i.e. with a very limited amount of springback from the 180° flat angle).

Table 3 Pressure and temperature ranges used in the flattening tests

		Stainless steel		Low carbon steel	Aluminium alloy	
Thickness t_0 (mm)		0.8	1.2	0.8	0.8	1.2
Dwelling pressure (MPa)	P_{min}	62	62	82	43	43
	P_{max}	691	950	320	900	730
Tool temperature (°C)	T_{hot}	n.a.		n.a.	293	
	T_{warm}	271		271	111	
	T_{room}	20		20	20	

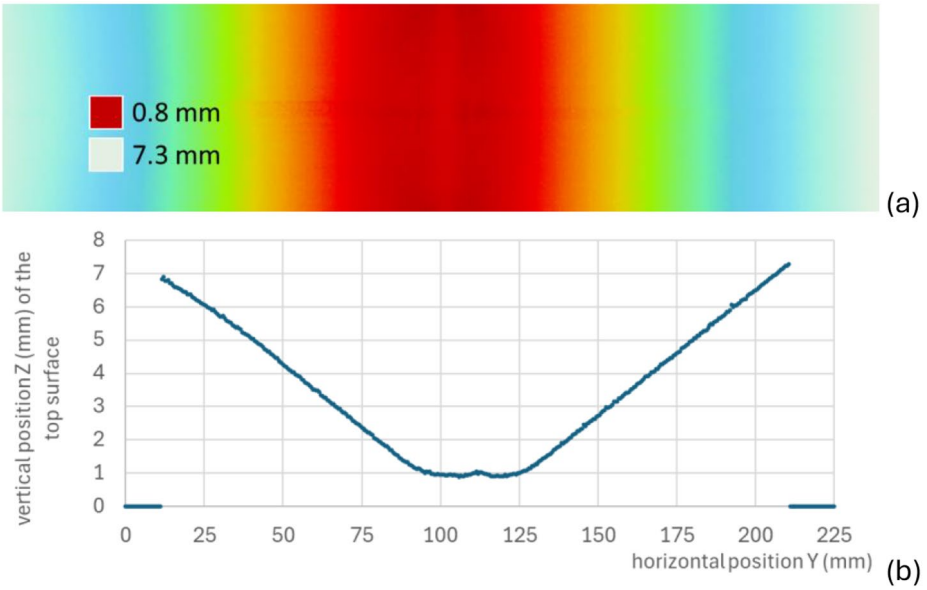

Fig. 6 (**a**) colormap scan of a 0.8 mm thick aluminium specimen flattened from an initial angle of $\alpha = 74.4°$ with flat tools at low pressure and low temperature T_{room}, exhibiting a strong springforward response; (**b**) longitudinal cross section profile of the scan, celrly showing an m-shaped profile at the center

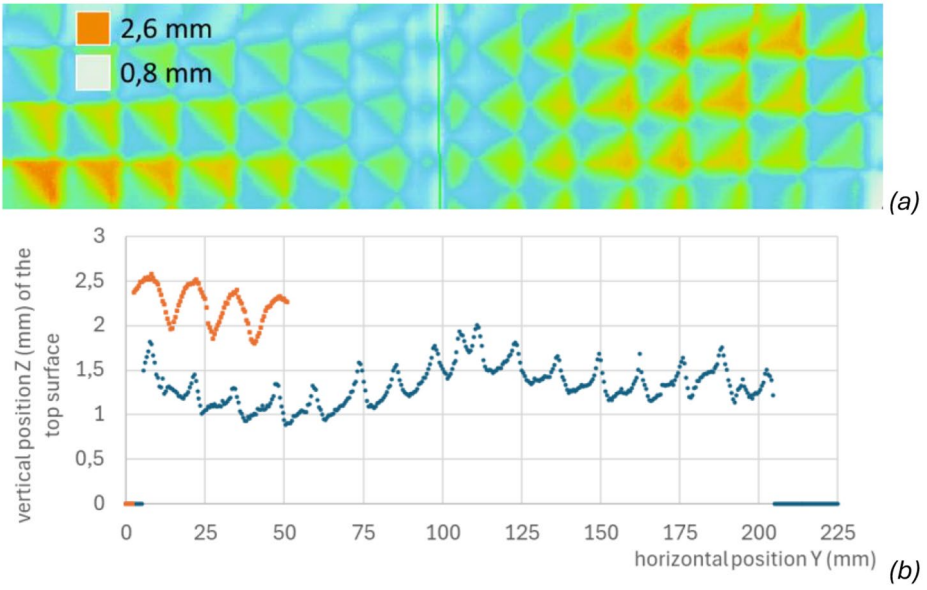

Fig. 7 (**a**) colormap scan of a 0.8 mm thick stainless steel specimen flattened at high pressure and low temperature T_{room}, with the top tools equipped with a steel mesh; (**b**) longitudinal and transverse cross section (at the centreline) profile of the scan

Experimental results

An extensive plan of bending and unbending experiments has been designed, using three different sheet materials. The independent factors which have been changed in the experimental plans have been presented in sect. "Materials and methods".

Some conditions have been replicated twice in order to assess the repeatability of the process. The total actual number of performed tests is 82. A statistical analysis of the result has been performed, trough linear regression with full factorial combination up to the third order interactions, with the statistical software JMP. The analysis has been performed separately for each material, for providing a simpler interpretation of the results. For all three regression models, all the factors are statistically significant, either directly or through an interaction.

Results with stainless steel

In Fig. 8, the results are shown for the stainless steel samples, in the form of coloured contour plots. The blue part of the plots locates the conditions where the final angle is around 180°±2°, i.e. nearly flat. The reddish part of the plots instead locates the springforward regions, where α_f>182°. Each plot is represented as a function of the variables α and P. The comparisons among the plots allows to appreciate the influence of the other factors. The factors that mostly influence the results are the initial angle, the temperature and the presence of a steel mesh.

Role of initial angle α. In all plots, there is a clear and relevant effect of the initial angle α, which is the most influential variable: as the initial angle gets smaller, the final angle

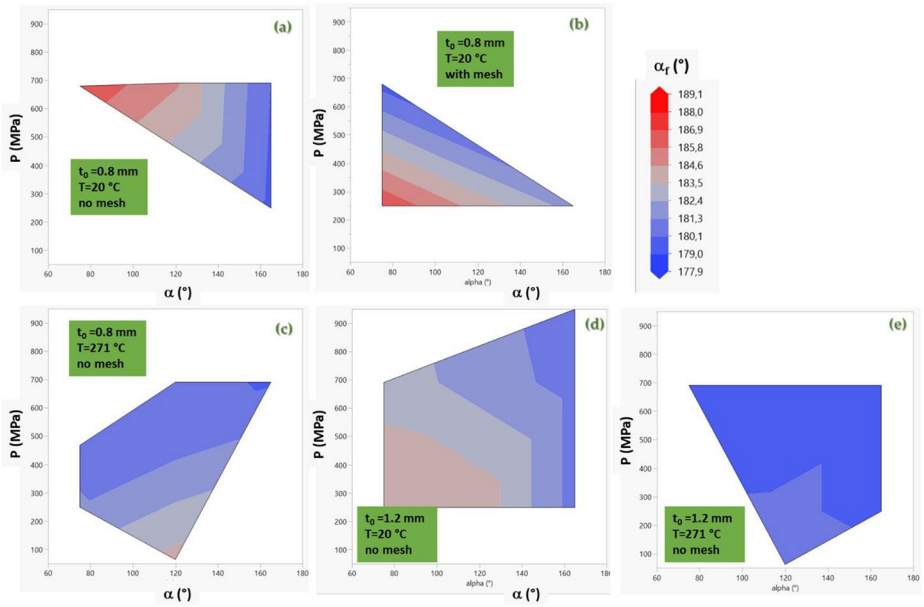

Fig. 8 Contour plots of the final angle vs. the initial angle α and the pressure P for the stainless steel samples

increases. The reason is that samples that have a smaller initial α are taller, and therefore experience a more pronounced bending effect (the one shown in Fig. 3a) while flattening and, as a result, will experience a more pronounced m-shaped profile and springforward after the load is released.

Role of tool temperature T. Heating the dies at a warm temperature for steel (271 °C) is sufficient to reduce the springforward: if we compare Fig. 8a and c we notice that the latter is almost entirely in the blue region. The sheet metal is positioned cold inside the tooling and in the flattening phase there are only 3 points of contact, with limited possibility of transferring heat from the tools to the sheet metal. Temperature displays its relevant softening effects during the dwelling phase, when there is full contact between the sheet and both top and bottom dies. Austenitic stainless steels decrease their strength already at warm temperatures, below 300 °C, as demonstrated by the scientific literature [37], and this behaviour can be exploited to improve formability and reduce elastic springback effects.

Role of superposing a steel mesh. The stress superposition provided by the steel mesh helps reducing the springforward (compare Fig. 8a and b). The springback and springforward suppression mechanism produced by the steel mesh, in interaction with the pressure P and the initial thickness t_0 is further discussed in Sect. 3.4. If pressing at room temperature and with no steel mesh (Fig. 8a and d), increasing the pressure P has almost no effect on the response. On the contrary, an interaction can be observed with temperature and with the use of a steel mesh: if pressing at high temperature (Fig. 8c and e) and/or pressing with the aid of a superposed steel mesh (Fig. 8b), it is possible to flatten better the samples by increasing P.

The role played by the initial thickness is generally very limited (compare Fig. 8a with Fig. 8d and compare Fig. 8c with Fig. 8e), but the results show that (surprisingly) it is easier to restore the part planarity of thicker rather than thinner sheet, at the same level of temperature and pressure, if no mesh is used. Indeed, having thicker sheets enhances the bending stiffness of the lateral flanges during the unbending (flattening) process, as illustrated in Fig. 3. The greater the thickness, the higher the bending stiffness, resulting in a larger curvature of the bent flange while flattening, which subsequently leads to reduced localization of plastic deformation at the edges of the bent line.

Even with thin sheets, deformation at the sides of the bent line can cause springback or springforward. This can be reduced by adjusting process parameters like temperature and pressure or using a grid to localize contact pressure and plastic deformation, improving planarity. Springback is influenced by factors such as material thickness, Young's modulus, prior plastic deformation, and material flow stress.

Results with aluminium alloy

In Fig. 9, the results are shown for the aluminium samples, using a different representation, to provide an alternative way of interpreting the multi-dimensional domain of the independent variables. T and α are the most influential parameters, along with the possible use of the steel mesh, as shown in the left part of the figure.

Role of initial angle α. Unsurprisingly, for larger values of the initial angle α of the bent sheet, the final α_f is closer to 180°, i.e. nearly flat in all conditions.

Role of tool temperature T. When the tool temperature is hot, at 293 °C, there is practically no springback nor springforward (Fig. 9e and f), for any value of the other conditions, being α_f=180°±2°. The most difficult condition is when pressing at room temperature

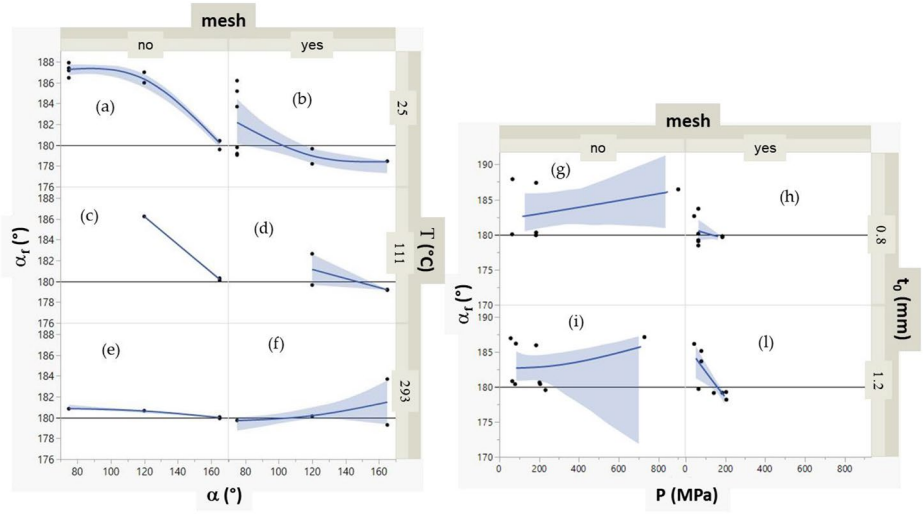

Fig. 9 On the left final angle α_f vs. the initial angle α, for different flattening die temperatures (T), with or without the mesh. On the right final angle α_f vs. the pressure applied (P) for two values of thickness tested, with and without mesh. In all the plots, most values are above 180°, i.e. they exhibit springforward. Data have been analysed through JMP (SAS Institute Inc.) in a scatter plot including as visible a regression model, where the band represents the confidence interval for the predicted values

samples that are initially bent at 75° or 120° (Fig. 9a and b). If pressing at warm temperature (111 °C), there is virtually no advantage over pressing at room temperature (compare Fig. 9a with Fig. 9c). The yield stress of the aluminium alloy 5754 does not change until the temperature overcomes 150 °C; at 200 °C, the yield stress decreases already of about 30% with respect to the room temperature condition, and this behaviour can be used to reduce springback and increase formability [38].

Role of superposing a steel mesh. If applying a steel mesh between the top die and the sheet, the amount of spring-forward is dramatically reduced (compare Fig. 9a and b).

Role of pressure P. A statistically significant effect is also given by the pressure P. If a steel mesh is used (Fig. 9h and l), it is easier to obtain a flat final shape if a larger dwelling pressure P is applied. With a steel mesh the sample become well flattened already at low pressure values, around 150 MPa or less. When a steel mesh is used, the superposed stress provided can easily suppress the springforward already at relatively low levels of pressure, and it is not advisable to increase the pressure because this generates aesthetical defects on the surface, as shown in Fig. 7. On the contrary, if no steel mesh is used (Fig. 9g and i), it is very difficult to suppress springforward (especially at room temperature) and the effect of pressure is negligible.

Role of initial thickness t_0. A minor effect is also given by the sheet thickness t_0. If using a steel mesh, it is easier to obtain a flat final shape for thinner samples (compare Fig. 9h and l). Without any mesh, the role of thickness is negligible, with a very small advantage with thicker samples (as already seen for the stainless steel).

Role of the sheet material. The regression models used for building the contour plots can also be used as a profiler, i.e. to predict the conditions (temperature and pressure) at which an angle of 180° can be obtained from a given v-bend specimen. An example is given in

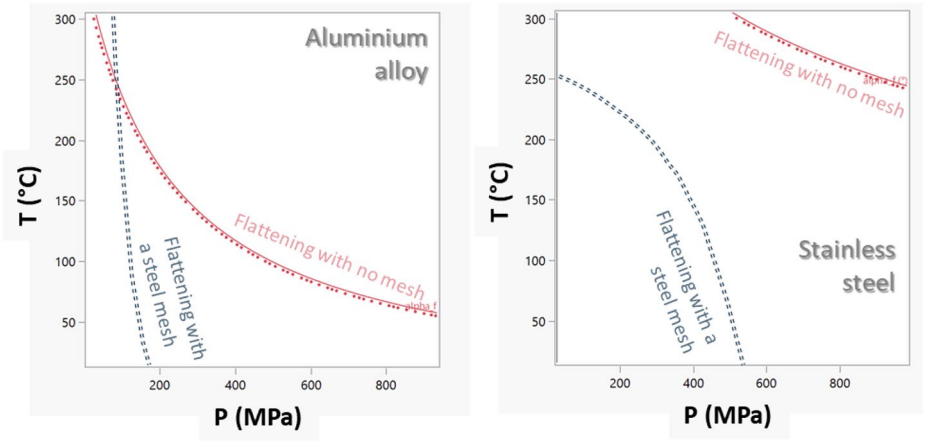

Fig. 10 Temperature and pressure conditions at which a 1 mm thick sample, pre-bent at 90°, can be completely flattened, with or without the superposition of a steel mesh

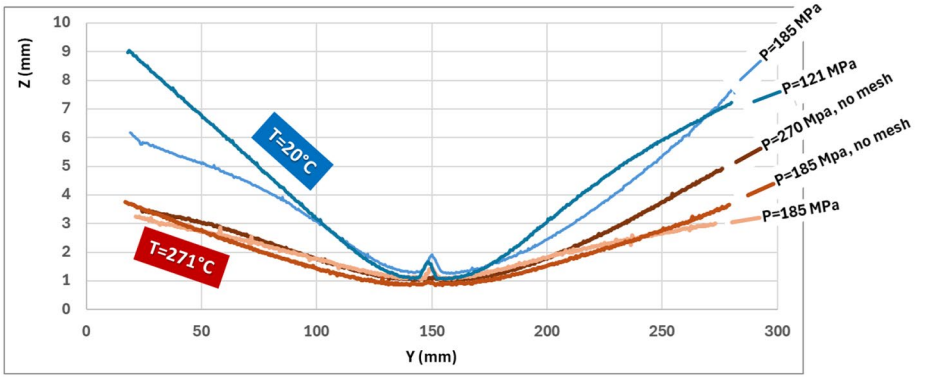

Fig. 11 Profiles of low carbon steel samples (t_0=0.8 mm) with initial mean α=100°, after flattening; three of them have been flattened superposing a steel mesh; blue lines represent samples flattened at room temperature, red lines represent the samples flattened at warm temperature. Note that the scale of the Y and Z axes is different, therefore the real profiles are much flatter than they appear

Fig. 10, which clearly shows that flattening an aluminium sample requires less pressure and less temperature of a stainless steel sample with the same initial dimensions.

Results with low carbon steel

If analysing the results obtained with the carbon steel samples, similar conclusions can be derived, as the ones reported above, with respect to the effect of all process parameters, although the data obtained with the DC04 samples present a larger variability, i.e. the statistical significance of the observations is lower.

An interesting observation can be done about the role of the temperature T, with reference to the next Fig. 11, where the final longitudinal profiles are shown, of samples bent to

an initial angle around α = 100°, then flattened. In the top part of the figure the profiles of samples flattened at room temperature (blue lines) are shown, with a larger springforward, with respect to the samples flattened at warm temperature. The role of pressure P and even the use of a steel mesh becomes almost negligible in the warm flattening operations, while P has some more effect for the cold flattening tests.

The beneficial effect of using warm tools is somehow surprising, because the scientific literature on the warm forming of automotive low carbon steels is extremely scarce. There is a general agreement that low carbon micro-alloyed steel might harden at warm temperature (below 400 °C) because of the precipitation of carbides, triggered by elements such as Vanadium, Chromium or others [39]. However, the DC04 steel used in the present paper includes no precipitation hardening elements, except for a very low fraction of chromium, less than 0,04% in weight. The softening effect of temperature thus prevails, which helps reducing elastic springback effects [40].

Interpretation and comparison of the experimental results

In order to interpret the data from the experiments more clearly, the main results for each material are summarized in a comparative table. This table highlights how the different process parameters—such as the initial bending angle (α), temperature (T), pressure (P), sheet thickness (t_0), and the use of a steel mesh—affect the final flatness of the samples. It allows us to see at a glance which factors are most influential and under which conditions the best results were obtained (see Table 4).

The different behaviors observed are primarily due to the material-specific properties, thermal sensitivity, and the interaction between thickness and process parameters.

- **Material-Specific Properties**

  Stainless steel, being stiffer than other materials tested, resists deformation more but also experiences more springback compared to softer materials like aluminium, which deforms more easily under pressure, especially at higher temperatures. Low carbon steel falls in between, showing variability due to its lower strength and slight hardening at warm temperatures.

- **Thermal Sensitivity**

  Aluminium softens more at lower temperatures (above 200 °C), reducing springback more effectively. Stainless steel and carbon steel require different temperature ranges to achieve similar effects.

- **Thickness and Process Interaction**

  Thicker sheets tend to resist deformation better and are easier to flatten with the correct process parameters, while thinner sheets are more prone to springback unless temperature and pressure are carefully adjusted.

Table 4 Comparison of the experimental results for different materials

	Initial Angle (α)	Temperature (T)	Steel Mesh	Pressure (*P*)	Thickness (t_0)	Summary of results
Stainless Steel	Smaller α → Increased springforward	Warm temperature (271 °C) reduces springforward	Reduces springforward, especially with high P	Higher P improves flattening with mesh and at high temperature	Thicker sheets flatten better at same P and T when no mesh is used	Initial angle greatly impacts flattening; heated dies reduce springforward, and mesh enhances results. Pressure significantly affects outcomes, especially with mesh and high temperatures. Thicker sheets flatten easier without mesh, being less prone to springback.
Aluminium Alloy	Larger α → Nearly flat final shape	Hot temperature (293 °C) eliminates springback	Dramatically reduces springforward	Higher P aids flattening with mesh; low P sufficient with mesh	Thinner sheets flatten better with mesh	Initial angle and temperature are the key factors. Steel mesh and heat reduce springback, with pressure being significant when using mesh. Thinner sheets flatten more easily with mesh.
Low Carbon Steel	Similar behavior to stainless steel	Warm temperature reduces springforward significantly	Mesh effect negligible at warm temperature	Higher P aids cold flattening; negligible effect at warm temperature	Minimal effect overall, similar to stainless steel	Temperature significantly reduces springforward, while pressure and mesh effects are more prominent during cold flattening. Warm tools are especially effective in minimizing elastic springback.

Discussion of the effects of using a steel mesh through numerical simulations

The complex effects that the presence of the steel mesh displays on the final process response is here discussed, in interaction with the other parameters, namely the pressure P and the initial thickness t_0. To this aim, FEM models of the process have been built.

Implicit FEA simulations were conducted using Transvalor FORGE software. From experimental plan, four bending-flattening conditions were chosen for simulations. The simulation plan followed is described in Table 5.

The tool sets used in the simulations are shown in the Fig. 12.

The materials have been modelled as isotropic, with no strain rate and no temperature effect, hence only some conditions at room temperature have been simulated. The strain hardening curve of the materials has been determined through their tensile properties, and modelled using a power law with only two coefficients:

$$\sigma = K\varepsilon^{n} \tag{5}$$

K is the consistency of the material, n defines the material's sensitivity to strain. In the simulations the sample materials were Aluminum and stainless steel AISI304. The K and n hardening coefficients are given in Table 6.

For simplicity no damage model was introduced in the simulations. Initially, all samples were meshed as "fine" automatically by using recommended value of the software. Remeshing on deformation was active with threshold value of 0,8. "Automatic and anisotropic adaptation" was preferred as remeshing mode which better suits large geometries with low thickness values. This was done to optimize simulation time without sacrificing accuracy. In this model, mesh numbers increase and become finer as the deformation occurs, taking into account given limitations such as maximum element size and maximum number of mesh number. An example of this remeshing technique is shown in Fig. 13.

Elastic springback of the sample was activated after each step. Lubrication condition was chosen from software database as "high" which uses Coulomb limited Tresca model with coefficients $\mu = 0{,}2$ and $\bar{\mu} = 0{,}4$.

The action of the steel mesh (modelled as rigid body) has been simplified, modelling the presence of parallel steel wires only in the Y direction, because this is the bending (and unbending) direction. The models use solid tetrahedral elements for the sheet and implicit time integration schemes, while the tools have been modelled as rigid bodies. Symmetry planes have been enforced to reduce the computational time.

The numerical results demonstrate that the presence of the steel mesh between the top die and the sheet completely changes the stress distribution on the metal part when the tools are in the dwelling phase. While it may seem intuitive that the stress on the sheet increases with the introduction of a steel mesh due to reduced contact area, the results reveal several critical implications. The increased stress facilitates improved flattening outcomes and reduces springback, as evidenced by the experiments. Moreover, the stress distribution throughout the sheet demonstrates how the mesh influences stress patterns, which can significantly affect performance during flattening.

In Fig. 14, the simulated Von Mises stress distribution during the dwelling phase (before load release) for two 0,8 mm thick aluminium samples pressed at room temperature is

Table 5 Simulated conditions

Run Name	Tool Set	Sheet Material	Bending Stroke (mm)	Flattening Conditions (Dwell Force (tonf), Dwell Time (s), Tool Temperature (C)
4	A	Al-alloy	5,945	250 tf, 10 s, 20 C, flat tools
34	B	AISI304	2,634	206 tf, 10 s, 20 C, flat tools
36	A	Al-Alloy	5,944	56 tf, 10 s, 20 C, with mesh tools
37	B	AISI304	2,634	78 tf, 10 s, 20 C, with mesh tools

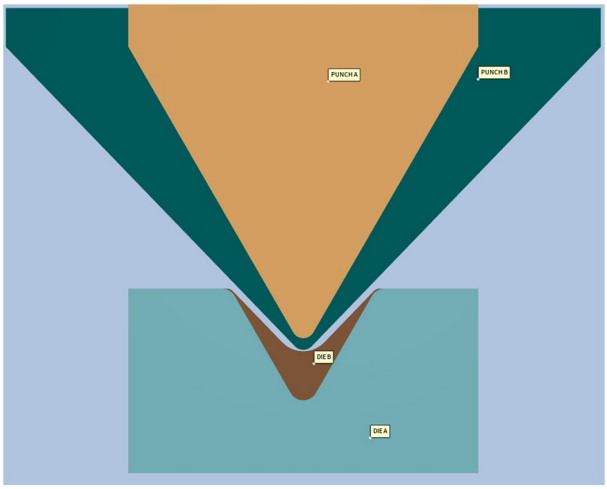

Fig. 12 Tool sets A and B

Table 6 Power law coefficients of used sample materials

Material	K (MPa)	*n*
Aluminum	354	0,18
AISI304	1478	0,24

shown. The sample on top is pressed with a very high average pressure of 900 MPa, but no steel mesh is used. The second sample on the bottom of the figure is pressed with a much lower pressure (185 MPa) but a steel mesh is used. It reaches higher maximum values of Von Mises stress, but concentrated where the steel wires are located. The experimental results of the two samples simulated in Fig. 14 confirm that, despite the very high dwelling pressure, a significant springforward occurs if no steel wire mesh is superposed. In other words, the numerical model, beyond mere observation, allows for the prediction of material behavior under varied conditions and enables the exploration of the effects of different process parameters. Additionally, the use of numerical modeling mitigates the challenges associated with experimental approaches, such as high costs.

In conclusion, the steel wires stiffen the material in the direction of bending and the sample practically experiences no springforward nor springback.

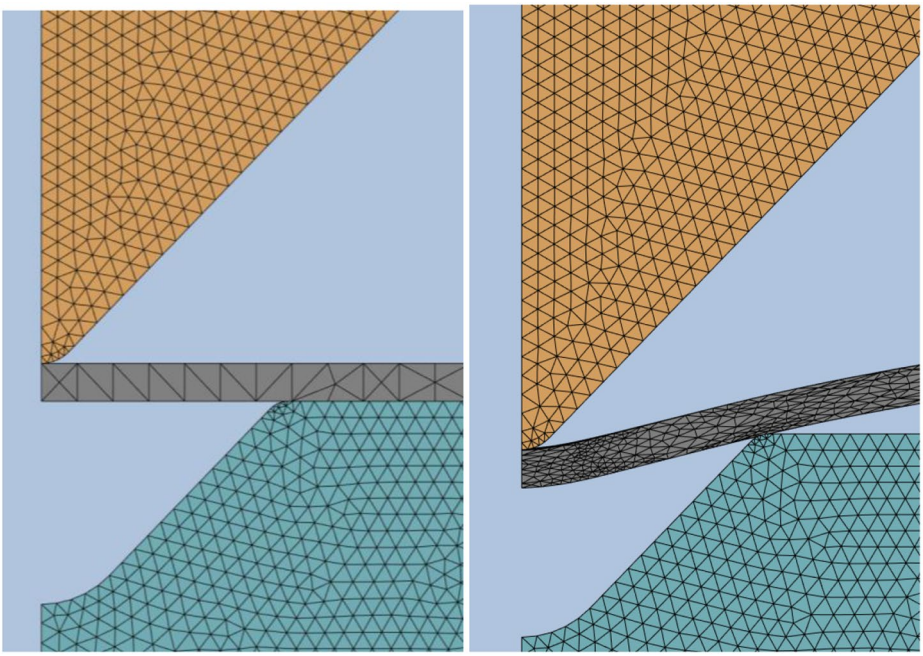

Fig. 13 Automatic and anisotropic remeshing technique for large thin parts in FEA simulations

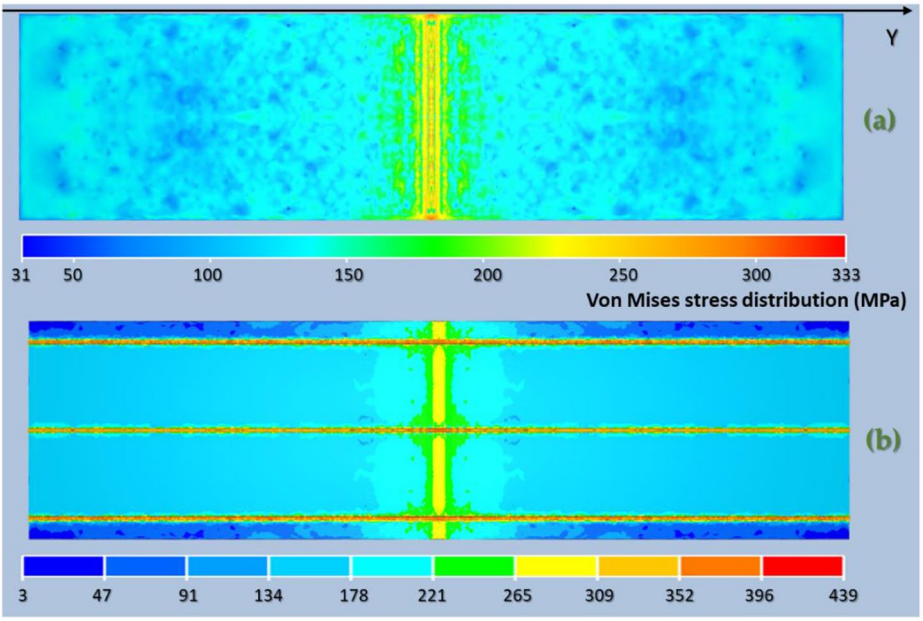

Fig. 14 Simulated Von Mises stress distribution during the dwelling phase for two aluminium samples with $t_0 = 0.8$ mm pressed at room temperature; the sample on top (**a**) is pressed with a very high average pressure of $P = 900$ MPa, but no steel mesh is used. The second sample (**b**) is pressed with a much lower pressure ($P = 185$ MPa) but a steel mesh is used below the top die

Conclusions

Flattening tests and simulations have been conducted on previously v-die bent samples made of stainless steel, low carbon steel and aluminium alloy.

The mechanics of the flattening process generally induces a springforward phenomenon, i.e. samples that where originally bent downward will eventually be mildly curved upward. The springforward can be suppressed under any of the following conditions:

- if the initial bend is very mild, e.g. angle α is, e.g. larger than 160°;
- or if the tools are heated up to a temperature above 270 °C;
- or if a steel mesh (which creates a superposition of local stresses) is applied between the top die and the sheet metal.

If none of the above conditions are met, it is virtually impossible to suppress the springforward, but it will be lower for materials with lower strength and when higher dwelling pressure values are applied.

The original material thickness greatly affects plastic deformation during forming and reforming. In bending (forming), thicker materials distribute stress more evenly, reducing localized deformation and the risk of defects, while thinner materials are more prone to concentrated deformation. During flattening (reforming), thicker materials experience less springback due to greater resistance, leading to more uniform deformation. Thicker sheets also produce larger curvatures during unbending, reducing edge deformation. This curvature is influenced by the initial bending angle, creating a strong link between forming and reforming stages.

The effects of thickness also depend on a material's mechanical properties, such as flow stress, Young's modulus, and deformation at yielding. These factors, along with the flow curve and previous deformation history, influence strain localization through the thickness, affecting springback or springforward. Experiments show that optimizing process parameters like temperature and pressure can further improve part planarity, enhancing the quality and efficiency of remanufacturing processes.

Lastly, when a steel wire mesh is superposed onto the sheet, the flattening effect improves for thinner sheet and for larger pressure values, but it is suggested to keep the dwelling pressure low for preserving the aesthetical quality of the sheet surface.

Author contributions M.S. wrote the manuscript and scientifically supervised and managed the research work. D.F. did the experimental work and reviewed the article. E.K. performed the numerical simulations.

Funding The study has been partly funded by the project "Accordo di collaborazione per la realizzazione di un'innovativa infrastruttura pilota regionale di supporto alla transizione verso l'economia circolare (DGR XI/4730 del 17/05/2021)", financed by the Lombardy Region and by the project "PON Ricerca e Innovazione 2014–2020 (CCI 2014IT16M2OP005), risorse FSE REACT-EU", financed by the Italian Ministero dell'Università e della Ricerca. The study has also been partly funded by the project RemaNet, under the call EU HORIZON-CL4-2023-TWIN-TRANSITION-01, Grant Agreement No. 101138627.

Data availability Experimental data will be provided upon request to the corresponding author.

Declarations

Competing interests The authors declare no competing interests.

References

1. Dumée LF (2022) Circular materials and Circular Design—Review on challenges towards Sustainable Manufacturing and Recycling. Circular Econ Sustain 2:9–23. https://doi.org/10.1007/s43615-021-00085-2
2. Kalverkamp M, Raabe T (2018) Automotive Remanufacturing in the Circular Economy in Europe. J Macromarketing 38:112–130. https://doi.org/10.1177/0276146717739066
3. Kurt A, Cung V-D, Mangione F et al (2019) An Extended Circular Supply Chain Model Including Repurposing Activities. In: 2019 International Conference on Control, Automation and Diagnosis (ICCAD). IEEE, pp 1–6
4. Duflou JR, Tekkaya AE, Haase M et al (2015) Environmental assessment of solid state recycling routes for aluminium alloys: can solid state processes significantly reduce the environmental impact of aluminium recycling? CIRP Ann 64:37–40. https://doi.org/10.1016/j.cirp.2015.04.051
5. Baffari D, Buffa G, Ingarao G et al (2019) Aluminium sheet metal scrap recycling through friction consolidation. Procedia Manuf 29:560–566. https://doi.org/10.1016/j.promfg.2019.02.134
6. Wagiman A, Mustapa MS, Asmawi R et al (2020) A review on direct hot extrusion technique in recycling of aluminium chips. Int J Adv Manuf Technol 106:641–653. https://doi.org/10.1007/s00170-019-04629-7
7. Li X, Baffari D, Reynolds AP (2018) Friction stir consolidation of aluminum machining chips. Int J Adv Manuf Technol 94:2031–2042. https://doi.org/10.1007/s00170-017-1016-4
8. Paraskevas D, Vanmeensel K, Vleugels J et al (2015) Solid state recycling of aluminium sheet scrap by means of spark plasma sintering. Key Eng Mater 639:493–498. https://doi.org/10.4028/www.scientific.net/KEM.639.493
9. Werner M, Haase R, Hermeling C (2023) reProd® – Resource-Autarkic Production Based on Secondary Semi-finished Products. In: Kohl H, Seliger G, Dietrich F (eds) Manufacturing Driving Circular Economy. GCSM 2022. pp 51–59
10. Farioli D, Fabrizio M et al (2023), Energy measurements and LCA of remanufactured automotive steel sheets. In: Materials Research Proceedings - ESAFORM 2023. Materials Research Forum LLC, Kraków, pp 1947–1956. https://doi.org/10.21741/9781644902479-210
11. Ingarao G, Zaheer O, Fratini L (2021) Manufacturing processes as material and energy efficiency strategies enablers: the case of single point Incremental forming to reshape end-of-life metal components. CIRP J Manuf Sci Technol 32:145–153. https://doi.org/10.1016/j.cirpj.2020.12.003
12. Ali AK, Wang Y, Alvarado JL (2019) Facilitating industrial symbiosis to achieve circular economy using value-added by design: a case study in transforming the automobile industry sheet metal waste-flow into Voronoi facade systems. J Clean Prod 234:1033–1044. https://doi.org/10.1016/j.jclepro.2019.06.202
13. Klett Y, Middendorf P, Sobek W Potential of origami-based shell elements as next-generation envelope components. In: 2017 IEEE International Conference on Advanced Intelligent, Mechatronics et al (2017) (AIM). IEEE, pp 916–920
14. Copani G, Shafinejad P, Hipke T et al (2022) New metals remanufacturing business models in automotive industry. Procedia CIRP 112:436–441. https://doi.org/10.1016/j.procir.2022.09.033
15. Brosius A, Hermes M, Ben Khalifa N et al (2009) Innovation by forming technology: motivation for research. IntJ Mater Form 2:29–38. https://doi.org/10.1007/s12289-009-0656-9
16. Abdullah ZT (2021) Assessment of end-of-life vehicle recycling: remanufacturing waste sheet steel into mesh sheet. PLoS ONE 16:1–17. https://doi.org/10.1371/journal.pone.0261079
17. Farioli D, Kaya E, Strano M (2024) Residual formability analysis of bent and remanufactured thin steel sheets. In: ESAFORM2024. Materials Research Forum, pp 1123–1134. https://doi.org/10.21741/9781644903131-124

18. Falsafi J, Demirci E, Silberschmidt VV (2016) Computational assessment of residual formability in sheet metal forming processes for sustainable recycling. Int J Mech Sci 119:187–196. https://doi.org/10.1016/j.ijmecsci.2016.10.013
19. Ueda T, Sentoku E, Wakimura Y, Hosokawa A (2009) Flattening of sheet metal by laser forming. Opt Lasers Eng 47:1097–1102. https://doi.org/10.1016/j.optlaseng.2009.07.002
20. Grüber M, Kümmel L, Hirt G (2020) Control of residual stresses by roller leveling with regard to process stability and one-sided surface removal. J Mater Process Technol 280:116600. https://doi.org/10.1016/j.jmatprotec.2020.116600
21. Farioli D, Fabrizio M, Kaya E et al (2023) Reshaping of thin steel parts by cold and warm flattening. IntJ Mater Form 16:35. https://doi.org/10.1007/s12289-023-01759-y
22. Galdos L, Mendiguren J, de Argandoña ES et al (2018) Influence of roll levelling on material properties and postforming springback. p 160008
23. Ahmadi M, Mohammad Sadeghi B, Arabi H (2017) Experimental and numerical investigation of V-bent anisotropic 304L SS sheet with spring-forward considering deformation-induced martensitic transformation. Mater Des 123:211–222. https://doi.org/10.1016/j.matdes.2017.03.040
24. Chatti S, Weinrich A, El Budamusi M et al (2015) Influencing the forming limits in air bending using incremental stress superposition. Key Engineering materials. Trans Tech Publications Ltd, pp 1602–1607
25. Briesenick D, Liewald M, Riedmueller KR (2021) New sheet metal forming process for springback reduction by continuous stress superposition. IOP Conf Ser Mater Sci Eng 1157:012030. https://doi.org/10.1088/1757-899x/1157/1/012030
26. Chatti S, Hermes M, Weinrich A et al (2009) New incremental methods for springback compensation by stress superposition. IntJ Mater Form 2:817–820. https://doi.org/10.1007/s12289-009-0613-7
27. Shinmiya T, Yamasaki Y, Miyake H, Hiramoto J (2022) Suppression of Springback for longitudinally curved part by Imparting In-Plane Compression Stress in Press Forming. Mater Trans 63:304–310. https://doi.org/10.2320/matertrans.P-M2021856
28. Mousavi A, Brosius A (2018) Improving the springback behavior of deep drawn parts by macro-structured tools. In: IOP Conference Series: Materials Science and Engineering. Institute of Physics Publishing
29. Wang JF, Wagoner RH, Matlock DK, Barlat F (2005) Anticlastic curvature in draw-bend springback. Int J Solids Struct 42:1287–1307. https://doi.org/10.1016/j.ijsolstr.2004.08.017
30. Radonjic R, Liewald M (2016) Approaches for springback reduction when forming ultra high-strength sheet metals. IOP Conf Ser Mater Sci Eng 159. https://doi.org/10.1088/1757-899X/159/1/012028
31. Birkert A, Hartmann B, Nowack M et al (2022) Advanced part design method for springback minimization of stamped sheet metal car body components. IOP Conf Ser Mater Sci Eng 1238:012082. https://doi.org/10.1088/1757-899x/1238/1/012082
32. Lee C-W, Yu J, Youn HW, Chung Y (2021) The Minimum Formable Radius of subtle feature lines in automotive outer panel stamping. Int J Autom Technol 22:993–1001. https://doi.org/10.1007/s12239-021-0089-0
33. Farioli D, Murgese L, Pinardi C et al (2024) Remanufacturing process chain for end-of-life aluminium car body parts: Technical and economic analysis. In: ESAFORM - Materials Research Proceedings 41. pp 2850–2860. https://doi.org/10.21741/9781644903131-312
34. Strano M, Semeraro Q, Iorio L, Sofia R (2018) Hierarchical metamodeling of the air bending process. J Manuf Sci Eng 140:1–34. https://doi.org/10.1115/1.4040025
35. Slota J, Šiser M (2016) Advanced Material models for Stamping of AW 5754 Aluminum Alloy. Strength Mater 48:487–494. https://doi.org/10.1007/s11223-016-9790-z
36. Ma B, Tieu AK, Lu C, Jiang Z (2002) A finite-element simulation of asperity flattening in metal forming. J Mater Process Technol 130–131:450–455. https://doi.org/10.1016/S0924-0136(02)00752-5
37. Hussaini SM, Krishna G, Gupta AK, Singh SK (2015) Development of experimental and theoretical forming limit diagrams for warm forming of austenitic stainless steel 316. J Manuf Process 18:151–158. https://doi.org/10.1016/j.jmapro.2015.03.005
38. Grèze R, Manach PY, Laurent H et al (2010) Influence of the temperature on residual stresses and springback effect in an aluminium alloy. Int J Mech Sci 52:1094–1100. https://doi.org/10.1016/j.ijmecsci.2010.04.008
39. Humphreys AO, Liu D, Toroghinejad MR et al (2003) Warm rolling behaviour of low carbon steels. Mater Sci Technol 19:709–714. https://doi.org/10.1179/026708303225002848
40. Ozturk F, Toros S, Kilic S (2009) Tensile and spring-back behavior of DP600 advanced high strength steel at warm temperatures. J Iron Steel Res Int 16:41–46. https://doi.org/10.1016/S1006-706X(10)60025-8